Laser Light Scattering Determination of the Surfactant Interface Thickness of Spherical Polystyrene Microlatices

Chi Wu

Department of Chemistry, The Chinese University of Hong Kong, Shatin, N.T., Hong Kong

Received June 24, 1994; Revised Manuscript Received August 23, 1994[⊗]

ABSTRACT: The core–shell structure of a spherical latex particle has been generally recognized, wherein a core usually made of cross-linked polymer chains is surrounded by a layer of small surfactant molecules. Our recent studies have revealed that the hydrophobic tails of the surfactant molecules partially penetrate into the polymer core. As a continuation of this work, the present study was designed to determine the degree of penetration. Polystyrene microlatices stabilized with cetyltrimethylammonium bromide (CTAB) were used as a model system in the investigation. A combination of both static and dynamic laser light scattering (LLS) results enabled us to determine the shell thickness to be ~(1.0 ± 0.2) nm, which indicates that about half of the CTAB hydrophobic tail penetrates into the polystyrene core since the fully stretched length of CTAB is about 2.7 nm. This degree of penetration has been confirmed by reanalyzing our previous LLS results on the same system with a newly modified structure of spherical microemulsions.

Introduction

The oil-in-water microemulsion polymerization can be used to make ultrafine microlatices with an average diameter in the range 5–50 nm.[1-3] The size of the microemulsion or final microlatices is normally related to the initial amount of monomer and surfactant.[3,4] The structure of microlatices can be generally described as a core–shell model, schematically shown in Figure 1, in which the polymer core is surrounded with a layer of small surfactant molecules adsorbed on its surface. Our recent studies showed that the average occupied surface area (s) per surfactant molecule on the surface of the polymer core is a fundamental parameter for governing the final size of microlatices.[5] In addition, our recent results also indicated that for a given experimental condition the surfactant molecules have a tendency to reach a closely packed state on the surface of the polymer core to minimize the interface energy between the hydrophobic core and the surrounding water. If a sufficient dispersion energy is supplied, the final radius (R) of microlatices can be predicted from the initial macroscopic weight ratio (W_m/W_s) of monomer to surfactant.

Figure 1 shows the hydrophobic tails of the surfactant molecules should be partially embedded inside the polymer core to form a surfactant/polymer interlayer because this condition is thermodynamically more favorable.[6] According to this picture, there exist three phases in this type of system: the polymer core (the "oil" phase), the water phase, and the surfactant interlayer phase. Therefore, the shell thickness b, if it is observable, should be less than the length of a fully stretched surfactant molecule. The important feature in this model is that the average occupied surface area per surfactant molecule (s) has been considered as a fundamental parameter to govern the size of microlatices.[5] There exists a lower limit for s because of the finite size of the surfactant molecule. At this limit, the core is completely covered. With these considerations, the following equation has been formulated:[5]

$$W_m/W_s = s\left(\frac{N_A\rho}{3M_s}\right)R + C \qquad (1)$$

The core-shell model of microlatex

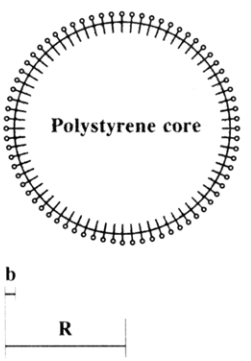

Figure 1. Schematic of a core–shell model for the structure of polystyrene microlatices, where R is the radius of the microlatices and b is the shell thickness.

where ρ, M_s, and N_A are the particle density, the molar mass of the surfactant molecule, and Avogadro's constant, respectively. C is a constant which remains to be explored in this study.

In this core–shell model, the hydrophobic tail of the surfactant molecule should partially penetrate into the polymer core. Naturally, we are not completely satisfied with this qualitative description of the core–shell structure but ask quantitatively to what degree this penetration should be, or in other words, the shell thickness b, which is related to the part of the surfactant molecules remaining outside the polymer core. It is known that this core–shell structure problem can be studied by small-angle neutron scattering.[7] However, a neutron source and a small-angle neutron scattering apparatus are not generally available. In this work, we have adopted a different experimental approach, namely, a combination of both static and dynamic laser light scattering (LLS), to study this core–shell structure.

Basic Theories

What Is the Constant C in Eq 1? According to the core–shell model presented in Figure 1, s equals the ratio of the total surface area (A_t) of the polymer core to the

[⊗] Abstract published in *Advance ACS Abstracts,* October 1, 1994.

0024-9297/94/2227-7099$04.50/0

total number of surfactant molecules ($N_A W_s/M_s$). A_t equals the surface area of one polymer core $[4\pi(R-b)^2]$ multiplied by the total number of microlatices $[(W_m + W_s)/(^4/_3\pi R^3\rho)]$, i.e.,

$$s = \left(\frac{[4\pi(R-b)^2](W_m + W_s)}{^4/_3\pi R^3\rho}\right)\Big/\left(\frac{N_A W_s}{M_s}\right)$$

or

$$\frac{W_m}{W_s} = s\frac{N_A\rho}{3M_s}\frac{R}{(1-b/R)^2} - 1 \qquad (2)$$

where ρ is the particle density. Since the typical ratio of b/R is normally less than 0.1, eq 2 can be rewritten as

$$\frac{W_m}{W_s} \cong s\frac{N_A\rho}{3M_s}R + s\frac{N_A\rho}{3M_s}(2b) - 1 \qquad (3)$$

where we have used the approximation of $(1-b/R)^{-2} \cong 1 + 2b/R$. After comparing eq 3 with eq 1, we have

$$C = s\frac{N_A\rho}{3M_s}(2b) - 1 \qquad (4)$$

which not only is a constant but also contains the information about the shell thickness (b).

Laser Light Scattering (LLS). In *static LLS*, the angular dependence of the excess absolute time-averaged scattered intensity, known as the excess Rayleigh ratio $[R_{vv}(\theta)]$, can be measured. For a dilute suspension at a concentration C (g/mL) and the scattering angle θ, $R_{vv}(\theta)$ can be approximately expressed as[8]

$$\frac{KC}{R_{vv}(\theta)} \cong \frac{1}{M_w}(1 + \langle R_g^2\rangle q^2) + 2A_2C \qquad (5)$$

where $K = 4\pi^2n^2(dn/dC)^2/(N_A\lambda_0^4)$ and $q = (4\pi n/\lambda_0)\sin(\theta/2)$ with N_A, dn/dC, n, and λ_0 being Avogadro's number, the specific refractive index increment, the solvent refractive index, and the wavelength of light *in vacuo*, respectively. M_w is the weight-average particle mass; A_2, the second-order virial coefficient; and $\langle R_g^2\rangle_z^{1/2}$, or simply R_g, the root-mean-square z-average radius of the particles. After measuring $R_{vv}(\theta)$ at a set of C and θ, we can determine M_w, R_g, and A_2 from a Zimm plot, which incorporates the dependence of $KC/R_{vv}(\theta)$ on both C and θ in a single grid.[8,9]

In *dynamic LLS*, an intensity–intensity time correlation function $G^{(2)}(n\Delta\tau,\theta)$ in the self-beating mode can be measured, which has the following form:[9,10]

$$G^{(2)}(t,\theta) = A[1 + \beta|g^{(1)}(t,\theta)|^2] \qquad (6)$$

where A is a measured baseline; β, a parameter depending on the coherence of the detection; t, the delay time; and $g^{(1)}(t,\theta)$, the normalized first-order electric field time correlation function. In general, $g^{(1)}(t,\theta)$ is related to the line-width distribution $G(\Gamma)$ by

$$g^{(1)}(t,\theta) = \int_0^\infty G(\Gamma)e^{-\Gamma t}\,d\Gamma \qquad (7)$$

The mostly accepted Laplace inversion program CONTIN[11] was used in this study to calculate $G(\Gamma)$ from the measured $G^{(2)}(t,\theta)$. Normally, Γ is a function of both C and θ[12] and is related to the translational diffusion coefficient D of particles by $\Gamma = Dq^2$.

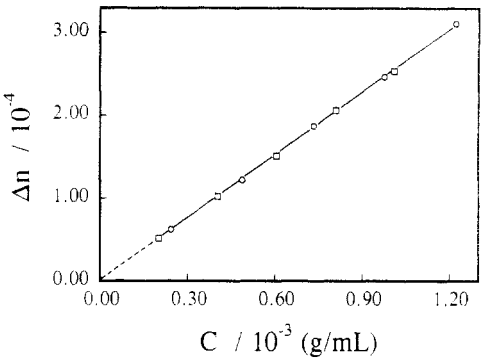

Figure 2. Plots of the refractive index increment (Δn) versus concentration (C) for S:CTAB-1 (○) and S:CTAB-2 (□) in water at 25 °C and 488 nm, respectively. The line represents an overall least-squares fitting of both the S:CTAB-1 and S:CTAB-2 data, which leads to a dn/dC value of 0.254 mL/g.

Experimental Section

Microemulsion Polymerization. For a typical microemulsion polymerization, 2 g of freshly distilled styrene, 10 mol % of cross-linker (*m*-diisopropenylbenzene), 50 mg of a lypophilic initiator (azobis(isobutyronitrile) (AIBN)), and a varied amount (0.04–6 g) of surfactant (cetyltrimethylammonium bromide (CTAB)) were added in distilled and deionized water to form a microemulsion with a total weight of 100 g. With a high-speed stirrer, we ensured that a sufficient dispersion energy was supplied. The details of synthesis can be found in refs 4 and 5. Two samples with respective styrene: CTAB ratios of 1:1 and 1:0.5 denoted hereafter as S:CTAB-1 and S:CTAB-2 were studied by both static and dynamic LLS and the rest were just studied by dynamic LLS.

LLS Instrumentation and Measurements. The microlatices were characterized at 25 °C by a commercial LLS spectrometer (ALV-5000, Langen in Hessen, Germany). An argon ion laser (Coherent INNOVA 90, operated at 488 nm and 100 mW) was used as the light source. The primary beam is vertically polarized. With a proper and special alignment, the present LLS spectrometer is capable of measuring the absolute scattered intensity in the scattering angle range of 6–154°, which is much wider than the range of a normal spectrometer. It is known that an accurate dn/dC value is vital for a good static LLS experiment. Recently, a novel differential refractometer was incorporated into our LLS spectrometer,[13] which enables us to precisely determine the values of dn/dC at identical conditions as LLS, such as the light wavelength and temperature. Therefore, an additional wavelength correction has been removed from our static LLS experiment. The details of the LLS instrumentation and its operation can be found elsewhere.[9]

Results and Discussion

Figure 2 shows plots of the refractive index increment (Δn) versus concentration (C) for S:CTAB-1 (○) and S:CTAB-2 (□) in water at 25 °C and 488 nm, respectively. *It should be noted that in the measurements of Δn water with the same amount of added surfactant as in the microemulsion was used as solvent so that the light intensity scattered by the surfactant molecules in S:CTAB-1 and S:CTAB-2 can be compensated.* By doing so, the possible influence or effects of surfactant molecules on the values of both dn/dC and M_w were removed experimentally. The measured dn/dC values for S:CTAB-1 and S:CTAB-2 are respectively 0.254 ± 0.002 and 0.253 ± 0.002 mL/g. The line in Figure 2 represents an overall least-squares fitting of the both S:CTAB-1 and S:CTAB-2 data, which leads to a dn/dC value of 0.254 mL/g. This dn/dC value is very close to the values in the literature for a similar polystyrene latex system.[14] With this dn/dC

Table 1. Summary of LLS Results of S:CTAB-1 and S:CTAB-2 at 25 °C[a]

sample	$10^{-7}M_w$	R_g (nm)	$10^8\langle D\rangle_z$ (cm²/s)	$\mu_2/\langle D\rangle_z^2$	R_h (nm)	R_g/R_h	R_{core} (nm)	b (nm)
S:CTAB-1	9.30	12.9	14.9	0.05	16.4	0.786	15.2	1.2
S:CTAB-2	28.5	19.0	9.57	0.05	25.5	0.779	24.4	1.1

[a] Errors: M_w, ±3%; R_g, ±5%; $\langle D\rangle_z$, ±1%; $\mu_2/\langle D\rangle_z^2$, ±10%.

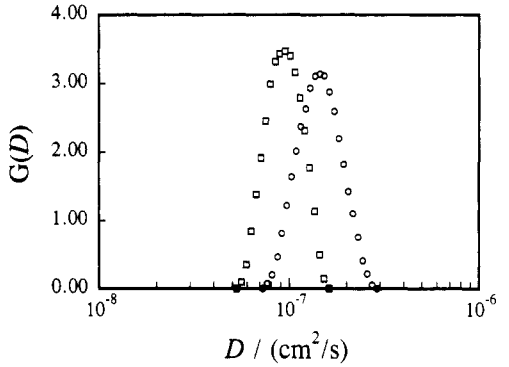

Figure 3. Translational diffusion coefficient distributions ($G(D)$) of S:CTAB-1 and S:CTAB-2 in aqueous suspension at 25 °C, which are the Laplace inversio of the corresponding measured time correlation functions. All distribution details are listed in Table 1.

value, we were able to carry out a precise static LLS experiment. The static LLS results (M_w and R_g) of S:CTAB-1 and S:CTAB-2 are summarized in Table 1. Since $[KC/R_{vv}(\theta)]_{\theta=0}$ is nearly independent of C, A_2 ($\sim -10^{-7}$ mol·mL/g²) is practically zero for both S:CTAB-1 and S:CTAB-2 in water at 25 °C.

Figure 3 shows the diffusion coefficient distributions ($G(D)$) of S:CTAB-1 and S:CTAB-2 in aqueous suspension at 25 °C, which are the Laplace inversion results of the corresponding measured time correlation fuctions. All distribution details, namely, the z-average diffusion coefficient, $\langle D\rangle_z = \int_0^\infty G(D)D\,dD$, and the distribution width, $\mu_2/\langle D\rangle_z^2 = [\int_0^\infty G(D)(D-\langle D\rangle_z)^2\,dD]/\langle D\rangle_z^2$, are also listed in Table 1. $\langle D\rangle_z$ can be further converted to the z-average hydrodynamic radius $(1/R_h)_z^{-1}$, or simply R_h, by the Stokes–Einstein equation, $D = k_BT/(6\pi\eta R_h)$, where k_B, T, and η are the Boltzmann constant, the absolute temperature, and the solvent viscosity, respectively. For convenience, the R_h values of S:CTAB-1 and S:CTAB-2 are listed in Table 1.

The R_g/R_h values of S:CTAB-1 and S:CTAB-2 shown in Table 1 are very close to the theoretical value (0.775) predicted for a uniform sphere, which directly indicates that the shape of the microlatices in both S:CTAB-1 and S:CTAB-2 are spheres with a uniform density. For a uniform sphere, it is known that its mass (M) can be related to its radius (R) by $M = (4/3)\pi R^3\rho$. After replacing M with M_w, we were able to calculate the radius of the polymer core (R_{core}) for both S:CTAB-1 and S:CTAB-2, which are also listed in Table 1. In the calculation, we have utilized the fact that the average density of cross-linked polystyrene microlatices is similar to that of bulk polystyrene ($\rho \sim 1.05$ g/cm³).[7] It should be mentioned that the calculated radius (R_{core}) was not greatly affected by some uncertainties associated with the chosen value of ρ since $R_{core} \propto \rho^{-1/3}$. According to the core–shell model, the shell thickness (b) can be estimated from the difference between the hydrodynamic radius (R_h) from dynamic LLS and the radius of the core (R_{core}) from static LLS. The values of b for S:CTAB-1 and S:CTAB-2 are 1.2 and 1.1 nm, respectively, which are also listed in Table 1.

Figure 4 shows a plot of $[R_h/(1 + W_m/W_s)]^{1/2}$ versus

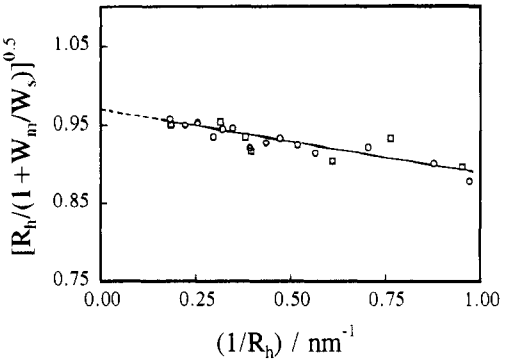

Figure 4. Plot of $[R_h/(1 + W_m/W_s)]^{1/2}$ versus $(1/R_h)$, where the circles and squares are the data from our laboratory and ref 4, respectively. The line represents a least-squares fitting of $[R_h/(1 + W_m/W_s)]^{1/2} = 9.67 \times 10^{-4}(1 - 0.794/R_h)$.

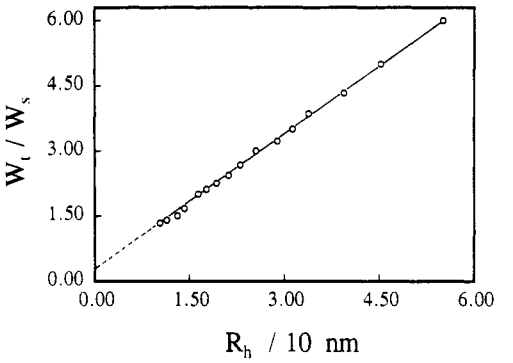

Figure 5. Plot of W_t ($=W_m + W_s$) versus R, where the circles are the data from our laboratory and the line represents a least-squares fitting of $W_t/W_s = 0.214 + 0.106R$.

$(1/R_h)$, where the circles and squares are the data from our laboratory and ref 4, respectively. The line represents a least-squares fitting of $[R_h/(1 + W_m/W_s)]^{1/2} = 9.67 \times 10^{-4}[1 - 0.794/R_h]$. The data presented in Figure 4 appear noisy. In fact, a close examination of the ordinate scale in Figure 4 shows that the actual noise is very small (<±2.5%). On the basis of eq 2

$$\left(\frac{RW_s}{W_s + W_m}\right)^{1/2} = \left(\frac{3M_s}{sN_A\rho}\right)^{1/2}(1 - b/R) \qquad (8)$$

A comparison of eq 8 with the least-squares fitting parameters gives us the value of $b = 0.794$ nm ≅ 0.8 nm.

Figure 5 shows a plot of W_t ($=W_m + W_s$) versus R_h, which is a reanalysis of the data in ref 5. The line represents a least-squares fitting of $W_t/W_s = 0.106R + 0.214$. On the basis of eq 2

$$\frac{W_t}{W_s} = s\frac{N_A\rho}{3M_s}R + s\frac{N_A\rho}{3M_s}(2b) \qquad (9)$$

It shows that the intercept/slope ratio in Figure 4 is $2b$; i.e., $2b = 0.214/0.106 = 2.02$ nm or $b \cong 1.0$ nm. In practice, eq 9 is more convenient and straightforward. The b values obtained from Figures 4 and 5 are slightly smaller than that calculated previously from S:CTAB-1 and S:CTAB-2. This might be attributed to the fact that the measured hydrodynamic radius (R_h) is normally larger than the actual particle radius (R) because of a possible hydrodynamically active hydration shell of the CTAB's polar end; i.e., the CTAB's hydrophilic heads are possibly associated with a layer of water molecules. It has to be emphasized that the calculation of b on the basis of eq 2 or 3 is not dependent on the precise value of either s or ρ.

Both our results and literature data show that the radius of the micelles formed with CTAB in water is about 2.45 nm, which is very close to the stretched full length of the CTAB molecule. In addition, our previous study has shown that the value of s is about 0.18 nm^2, which is close to the cross-section area of the CTAB molecule.[5] Therefore, we can conclude that statistically the CTAB molecules are straight on (or, "perpendicular to") the surface with a relatively rigid chain conformation. About half of the CTAB molecule penetrates inside the particle.

Conclusion

A set of cross-linked polystyrene microlatices prepared by an oil-in-water microemulsion polymerization have been successfully analyzed by laser light scattering on the core–shell structure model. After carefully removing the scattered intensity from the surfactant molecules, we have accomplished the characterization of the shell thickness by a combination of static and dynamic LLS results, i.e., the core radius from the weight-average particle core mass obtained in static LLS and the particle radius from the translational diffusion coefficient obtained in dynamic LLS. The shell thickness obtained in this way has been confirmed with the reanalysis of our previous results and existing data in the literature. Thus, we are able to conclude that the shell thickness in our studied microlatices is 1.0 ± 0.2 nm. This clearly indicates that in the core–shell structure model about half of the hydrophobic tail of the surfactant molecule penetrates into the polystyrene core and the other half together with the hydrophilic head of the surfactant molecule sticks out of the polymer core into the water.

Acknowledgment. The financial support of this work by the RGC (the Research Grants Council of the Hong Kong Government) Direct Grant 1993/94 (CUHK 220600390) is gratefully acknowledged.

References and Notes

(1) Guo, J. S.; El-Aasser, M. S.; Vanderhoff, J. W. *J. Polym. Sci., Polym. Chem. Ed.* **1989**, *27*, 691.
(2) Jayakrishnan, A.; Shah, D. O. *J. Polym. Sci., Polym. Lett. Ed.* **1984**, *22*, 31.
(3) Ferrick, M. R.; Murtagh, J.; Thomas, J. K. *Macromolecules* **1989**, *22*, 1515.
(4) Antonietti, M.; Bremser, W.; Schmidt, M. *Macromolecules* **1990**, *23*, 3796.
(5) Chi, Wu *Macromolecules* **1994**, *27* (1), 298.
(6) Sperling, L. H.; Klein, A.; Yoo, J. N.; Kim, K. D.; Mohammadi, N. *Polym. Adv. Technol.* **1990**, *1*, 263 and references therein.
(7) *Uniform Latex Particles*, 4th ed.; Seradyn Inc.: Indianapolis, IN, 1987.
(8) Zimm, B. H. *J. Chem. Phys.* **1948**, *16*, 1099.
(9) Chu, B. *Laser Light Scattering*, 2nd ed.; Academic Press: New York, 1991.
(10) Pecora, R. *Dynamic Light Scattering*; Plenum Press: New York, 1976.
(11) Provencher, S. W. *Biophys. J.* **1976**, *16*, 29; *J. Chem. Phys.* **1976**, *64*, 2772; *Makromol. Chem.* **1979**, *180*, 201.
(12) Stockmayer, W. H.; Schmidt, M. *Pure Appl. Chem.* **1982**, *54*, 407; *Macromolecules* **1984**, *17*, 509.
(13) Wu, C.; Xia, K. Q. *Rev. Sci. Instrum.* **1994**, *65* (3), 587.
(14) Chan, F. S.; Coring, D. A. *Can. J. Chem.* **1966**, *44*, 725.